

Article

Combining Rare Earth Element Analysis and Chemometric Method to Determine the Geographical Origin of Nephrite

Yue Su ^{1,2,*}  and Mingxing Yang ^{1,2,*}¹ Gemmological Institute, China University of Geosciences, Wuhan 430074, China² Hubei Province Gem and Jewelry Engineering Technology Research Center, Wuhan 430074, China

* Correspondence: gemlabmem@163.com (Y.S.); yangc@cug.edu.cn (M.Y.)

Abstract: Nephrite is a high-valued gem material, whose geographical origin determination is a topic of interest to both consumers and producers since the geographic origin determines its price and reputation. In the present study, we suggest a two-step method for discriminating geographical origins of nephrite based on the rare earth element (REE) contents combined with chemometrics. In the first step, the REE contents of nephrite samples were determined by laser ablation-inductively coupled plasma mass spectrometry (LA-ICP-MS), combined with previously reported data—the chondrite-normalized REE distribution pattern; the REE parameters of nephrite samples from six origins, namely Xinjiang, Qinghai, Russia, Guangxi, Guizhou, and Liaoning were then compared. In the second step, origin discriminant models were established by linear discriminant analysis (LDA), and the accuracy of the model was evaluated by leave-one-out cross-validation (LOOCV). The results showed that the REE contents were significantly different among the six nephrite origins with regional characteristics, which makes it possible to trace the origin. Using chondrite-normalized REE distribution patterns, the six nephrite origins can be divided into three separate groups: Xinjiang–Qinghai–Russia, Luodian–Dahua, and Xiuyan. Xiuyan nephrite can be directly distinguished from the other origins due to its unique REE distribution pattern. In the second step, the LDA discrimination models were performed on the remaining two groups. For the Luodian–Dahua group, the accuracy of the original classification and LOOCV were 97.9% and 85.4%, which indicated REE combined with LDA could effectively identify Luodian nephrite and Dahua nephrite. For the Xinjiang–Qinghai–Russia group, the accuracy of the original classification and LOOCV was 74.1% and 63.9%, respectively. Overall, this work proves that a combination of REE analysis and chemometrics has a certain feasibility and broad application prospects for geographical origin, and the same methodology can be applied to study the origin of other gem materials.



Citation: Su, Y.; Yang, M. Combining Rare Earth Element Analysis and Chemometric Method to Determine the Geographical Origin of Nephrite. *Minerals* **2022**, *12*, 1399. <https://doi.org/10.3390/min12111399>

Academic Editor: Donatella Barca

Received: 12 September 2022

Accepted: 28 October 2022

Published: 31 October 2022

Publisher's Note: MDPI stays neutral with regard to jurisdictional claims in published maps and institutional affiliations.



Copyright: © 2022 by the authors. Licensee MDPI, Basel, Switzerland. This article is an open access article distributed under the terms and conditions of the Creative Commons Attribution (CC BY) license (<https://creativecommons.org/licenses/by/4.0/>).

Keywords: nephrite; rare earth element; laser ablation-inductively coupled plasma mass spectrometry; linear discriminant analysis; origin determination

1. Introduction

Nephrite is a type of almost monomineralic rock containing tremolite ($\text{Ca}_2\text{Mg}_5\text{Si}_8\text{O}_{22}(\text{OH})_2$)–actinolite ($\text{Ca}_2(\text{Mg}, \text{Fe}^{2+})_5\text{Si}_8\text{O}_{22}(\text{OH})_2$) as its main components. Meanwhile, nephrite is a precious variety of gem material that is long cherished by Chinese people and plays an important role in Chinese jade culture. The nephrite currently in circulation in the jewelry market is mainly from Southern Xinjiang (Xinjiang Uygur Autonomous Region, China) [1–3], Golmud (Qinghai province, China) [4,5], Baikal (Russia) [6,7], and Chuncheon (South Korea) [8], with other economically valuable nephrite sources in China such as Xiuyan (Liaoning province) [9,10], Dahua (Guangxi province) [11,12], and Luodian (Guizhou province) [13]. Nonetheless, nephrite from Xinjiang is the most valuable (due to its superior material properties as well as its long reputation) [14]. The origin of nephrite is of great importance in the gem trade, as its value varies greatly depending on where it

comes from. Unscrupulous traders often sell nephrite from low-value sources as high-value sources, causing serious market disruption.

In gemmology, geographical origin identification of nephrite is a key subject of research, and the following factors contribute most to inaccurate geographical origin identifications: (1) high-quality nephrite from different origins is composed of almost pure tremolite (up to 99% tremolite), with few characteristic inclusions and very similar or extensive data overlap in physicochemical properties (e.g., color, luster, transparency, refractive index, specific gravity, main chemical composition) and spectroscopic characteristics (e.g., infrared spectroscopy, Raman spectroscopy, and UV-visible spectroscopy). (2) Nephrite deposits are widely distributed throughout East Asia, the ore-forming genesis is essentially the same in most cases, and the continuous emergence of new nephrite occurrences adds to the difficulty of determining origin.

Many attempts were devoted to differentiating nephrite origin, with representative papers mainly using different analytical methods (LA-ICP-MS) [15], laser-induced breakdown spectroscopy (LIBS) [16,17], Multispectral imaging [18], Raman spectroscopy [19], Near-infrared spectroscopy [20], Terahertz Spectroscopy [21], stable isotopes [22], etc., assisted with multiple statistical methods to achieve the differentiation of origin. In terms of sample size and differentiation results, origin determination still faces major limitations.

Rare earth elements (REE, thereafter) are a special group of trace elements; there are 15 metallic chemical elements with atomic numbers 57–71, from lanthanum through lutetium. All REEs have very similar physical and chemical properties and tend to occur in groups in geological bodies, making them good geochemical tracers of various geological interactions. REE composition patterns, REE ratios, and various parameters such as Eu and Ce anomalies are commonly used to trace the geochemical differentiation effect and indicate the genesis of various rock types [23]. LA-ICP-MS is a fast, simple, and highly accurate method that can effectively measure rock samples for REEs [24]. Since the laser vaporizes only a microscopic amount of the sample for analysis, laser ablation allows ICP-MS to be used on gemstones with minimal damage and does not affect the appearance of a gemstone, which made it ideal for gem testing [25]. The study of origin tracing based on REEs was fruitful, especially in the study of food (tea [26], wine [27], olive oil [28], pumpkin seed oil [29], milk [30], honey [31], etc.) and culture heritage [32–34]; it was, however, less often applied to highly valued mineral products, such as precious gemstone [35,36].

This work aims to verify the feasibility of differentiating the geographical origin of nephrite with an approach using the chondrite-normalized REE patterns and LDA. As a first step, using LA-ICP-MS for the determination of the REE concentrations in nephrite, coupled with reported data from published references, a total of 174 data points covering six nephrite origins were summarized and analyzed. Chondrite-normalized REE patterns were then used to explore the natural grouping of nephrite origins. Next, the nephrite samples in each group were further differentiated by LDA. Most importantly, the behaviors of natural grouping by chondrite-normalized REE patterns and the performance of the discriminant model were discussed with special emphasis on the relationship between the REE characteristics of nephrite and its ore-forming environment.

2. Materials and Methods

2.1. Samples

A total of 88 nephrite samples were examined for REEs measurement from three locations: Xinjiang, Qinghai, and Russia. Therein, 61 samples came from the counties of Yutian and Qiemo in Xinjiang, China; 12 samples were from the Sanchahe deposit in Golmud in Qinghai, China; and 15 samples came from the Lake Baikal region, Russia. All samples were directly collected during the fieldwork. To meet the requirements of measurements, all the collected rough samples were fashioned into cubic slabs (size: 3 cm × 1.5 cm × 0.5 cm) with well-polished surfaces (8000 mesh diamond grinding wheel polishing). Before the LA-ICP-MS measurement, infrared transform infrared spectroscopy (FTIR) verified all the research samples to be nephrite. To ensure the accuracy of acquired data, the in-situ

measurement was performed on a polished surface that was homogeneous in appearance, avoiding any visible impurity minerals, fissures, growth tubes, and diagnosis features such as “water lines” by checking under a reflection microscope.

Furthermore, the REE data of the nephrite samples from Luodian in Guizhou, Xiuyan in Liaoning, Dahua in Guangxi, and Golmud in Qinghai were cited from previously published literature, combined with our test data; a total of 174 data points were enrolled to analyze in this study. All these data were examined by ICP-MS or LA-ICP-MS. A description of the data set is shown in Table 1. Detailed information about individual analysis can be found in Supplementary Table S1. The locations of the nephrite deposits reviewed in this study and the appearances of representative nephrite samples for LA-ICP-MS measurement are shown in Figure 1.

Table 1. Test data and reference data for nephrite in this study.

Origin	Test Data (This Study)	Reference Data	Total Number	Reference
Xingjiang	61	0	61	-
Qinghai	12	20	32	Yu (2016) [37]; Ling et al. (2009) [38]; Ling et al. (2011) [39]
Baikal (Russia)	15	0	15	-
Luodian (Guizhou)	0	31	31	Liao and Zhi (2017) [40]; Zhang et al. (2015) [41]; Li et al. (2014) [42]
Xiuyan (Liaoning)	0	18	18	Che et al. (2013) [43]
Dahua (Guangxi)	0	17	17	Wang et al. (2007) [10]
Total	88	86	174	Wang et al. (2016) [11] -

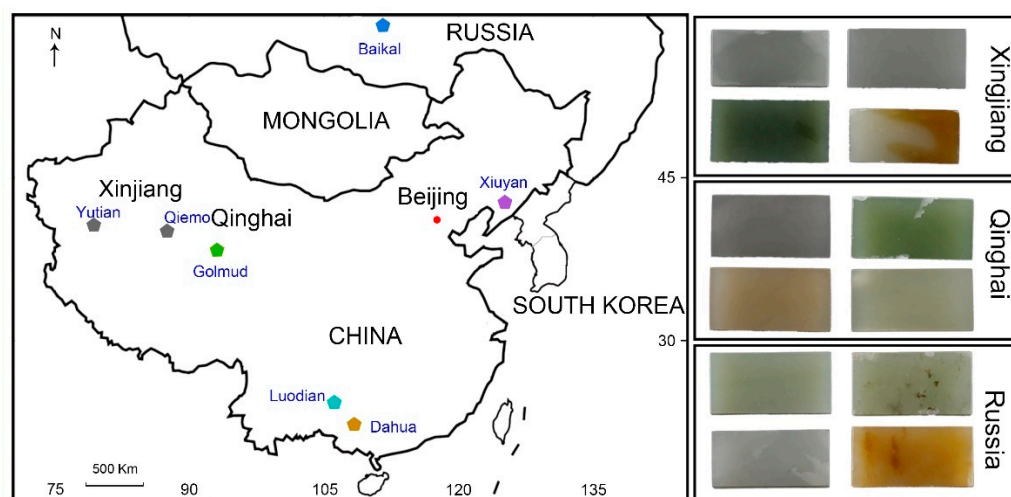


Figure 1. Locations of nephrite deposits investigated in this study are listed in the left-hand row. Photos of representative 3.0 cm × 1.5 cm cut nephrite samples for measurement are listed in the right-hand row.

2.2. Experimental Methods

Analyses were performed on a laser ablation-inductively coupled plasma mass spectrometry (LA-ICP-MS) at the Wuhan SampleSolution Analytical Technology Co., Ltd., Wuhan, China. The GeolasPro laser ablation system consists of a COMPexPro 102 ArF excimer laser (wavelength of 193 nm with maximum energy of 200 mJ) coupled with a MicroLas optical system. An Agilent 7900 ICP-MS instrument was used to acquire ion-signal intensities. The ablation aerosols were carried to the ICP-MS by Helium gas with a flow rate of 1.0 L/min. The spot size, laser energy, and repetition rate of the laser were

set to 44 μm , 6 J/cm², and 5.5 Hz, respectively. Every eight analyses were followed by a calibration process with two analyses of NIST 610 to correct the time-dependent drift of sensitivity and mass discrimination. A total of 45 elements were measured simultaneously by LA-ICP-MS. Trace element compositions of minerals were calibrated against various reference materials (BHVO-2G, BCR-2G, and BIR-1G) and ²⁹Si was chosen as the normalization element to calibrate all elemental concentrations. Each analysis incorporated a background acquisition of approximately 20 s followed by 50 s of data acquisition from the sample. An Excel-based software ICPMSDataCal was used to perform offline selection and integration of background and analyzed signals, time-drift correction, and quantitative calibration for trace element analysis [44].

Several factors can affect the results and interpretation of the measurements. Firstly, considering the matrix effect, any matrix differences between glass reference materials and tremolite crystal structure are consistent across the data sets, so they do not affect interpretation of results. Secondly, interference of polyatomic ions is the major factor affecting the precision of REE measurement, especially the interferences from oxides and hydroxides in light REEs. The interference imposed in LA-ICP-MS measurements can produce M²⁺ ions in ICP-MS and ¹⁵⁰Nd²⁺, ¹⁵⁰Sm²⁺, and ¹⁵⁶Gd²⁺ can cause significant interference when doubly charged by ⁷⁵As and ⁷⁸Se. Since the content of As and Se within nephrite is generally low (often <1 ppm), they barely interfere with dimers and trimers.

2.3. Data Processing

The REE data acquired from LA-ICP-MS measurement were reported as mean values \pm standard errors. In this study, statistical analysis was completed using SPSS statistics 22.0 analysis software from IBM, USA. The Kolmogorov–Smirnov test, Levene’s chi-square test, Kruskal–Wallis multiple comparative analysis, and linear discriminant analysis (LDA) were conducted to examine the difference in REEs from different nephrite origins. The Kolmogorov–Smirnov test for the normal distribution of 14 REEs from six origins revealed that although the data from multiple origins met independence, the data for REEs did not all meet normal distribution, and the Levene’s chi-square test also indicated that the variance of each origin grouping was not uniform, so the commonly used analysis of variance (ANOVA) was not suitable for this analysis. Thus, the Kruskal–Wallis method of non-parametric testing with multiple independent samples was used to determine whether there was a significant difference in the content of REEs between the different origins.

Linear discriminant analysis (LDA) is a supervised machine learning technique. LDA performs the separations in a linear direction, minimizing within-class variance while maximizing between-class variance. In 1936, the Linear Discriminant was firstly proposed by Ronald A. Fisher and later proved to be a useful classifier [45]. In this study, LDA was used to establish the origin discriminant model based on REEs. The spatial separation of sample sets in the discriminant space was visualized by score scatters of discriminant functions. The discriminant model was validated using leave-one-out cross-validation (LOOCV).

Masuda–Coryell diagrams, also known as standardized diagrams for chondrite, are utilized in geochemical studies of REEs, where different geological bodies with different origins, types, or locations have different rare earth partitioning patterns [46]. The REE contents of nephrite were normalized to REE concentrations of chondritic meteorites to eliminate the abundance variation between REEs of odd and even numbers caused by the Oddo–Harkins effects [47] and to reduce the fractionation of REEs.

In previous studies, scholars used different normalized reference protocols (including Masuda (1973) [46], Evensen (1978) [48], Boynton (1984) [49], Taylor and McLennan (1985) [50], etc.); in this study, we uniformly adopt the REE concentrations of chondrite reported by Sun and McDonough (1989) [51] as the normalization reference system. In addition, relevant parameters, such as the total abundances of REE (ΣREE), the ratio of LREE and HREE (LREE/HREE), the ratio of lanthanum and samarium ((La/Sm)_N), the

ratio of gadolinium and lutetium ($(\text{Gd}/\text{Lu})_N$), europium anomalies (δEu), and cerium anomalies (δCe). The Ce and Eu anomalies were calculated using the following equations:

$$\delta\text{Eu} = \text{Eu}_N / \sqrt{\text{Sm}_N * \text{Gd}_N} \quad (1)$$

$$\delta\text{Ce} = \text{Ce}_N / \sqrt{\text{La}_N * \text{Pr}_N} \quad (2)$$

3. Results and Discussion

3.1. Characteristics of the Rare Earth Elements in Nephrite from Different Origins

The characteristics of the contents and related parameters of REEs of different origins are shown in Table 2. In the Kruskal–Wallis test for multiple independent samples in the non-parametric test for REEs, the original hypothesis was that REEs are equally distributed over the six nephrite origins; the results show that the asymptotic significance value $p < 0.001$ for all REEs, so the original hypothesis is rejected. It can be concluded that there is a significant difference in the content of REEs for the six different origins.

Table 2. Contents of rare earth elements of nephrite of different origins.

Rare Earth Element	Xingjiang (n = 61)	Qinghai (n = 32)	Mean ± Standard Deviation (ppm)				Dahua (n = 17)	H Value, Significance *
			Russia (n = 15)	Luodian (n = 31)	Xiuyan (n = 18)			
La	0.994 ± 0.794	0.704 ± 0.961	0.734 ± 0.807	9.793 ± 7.040	12.093 ± 7.631	3.802 ± 2.242	115.334 *	
Ce	2.010 ± 1.609	1.981 ± 3.130	1.536 ± 1.020	5.178 ± 3.854	18.970 ± 10.846	1.811 ± 1.152	79.989 *	
Pr	0.267 ± 0.200	0.289 ± 0.547	0.203 ± 0.136	1.873 ± 1.106	2.088 ± 1.135	0.775 ± 0.450	106.171 *	
Nd	1.165 ± 0.740	1.323 ± 2.568	1.012 ± 0.702	7.085 ± 3.859	5.303 ± 3.011	3.032 ± 1.669	102.140 *	
Sm	0.343 ± 0.263	0.330 ± 0.541	0.255 ± 0.162	1.317 ± 0.645	0.549 ± 0.307	0.755 ± 0.365	79.754 *	
Eu	0.026 ± 0.022	0.050 ± 0.086	0.037 ± 0.044	0.302 ± 0.121	0.117 ± 0.082	0.149 ± 0.082	106.881 *	
Gd	0.446 ± 0.324	0.294 ± 0.302	0.380 ± 0.241	1.241 ± 0.545	0.581 ± 0.313	0.769 ± 0.283	79.792 *	
Tb	0.082 ± 0.070	0.051 ± 0.067	0.063 ± 0.063	0.193 ± 0.095	0.121 ± 0.068	0.121 ± 0.041	68.366 *	
Dy	0.569 ± 0.539	0.325 ± 0.373	0.453 ± 0.516	1.065 ± 0.509	0.802 ± 0.470	0.745 ± 0.262	60.978 *	
Ho	0.145 ± 0.162	0.059 ± 0.063	0.105 ± 0.132	0.216 ± 0.108	0.182 ± 0.113	0.167 ± 0.065	59.343 *	
Er	0.439 ± 0.520	0.173 ± 0.172	0.452 ± 0.630	0.597 ± 0.325	0.592 ± 0.349	0.478 ± 0.196	56.118 *	
Tm	0.066 ± 0.097	0.025 ± 0.025	0.083 ± 0.123	0.080 ± 0.047	0.093 ± 0.063	0.067 ± 0.030	46.436 *	
Yb	0.436 ± 0.711	0.189 ± 0.150	0.688 ± 1.436	0.425 ± 0.261	0.616 ± 0.390	0.410 ± 0.183	38.005 *	
Lu	0.063 ± 0.096	0.028 ± 0.025	0.144 ± 0.323	0.060 ± 0.040	0.091 ± 0.072	0.050 ± 0.022	30.347 *	
ΣREE	7.050 ± 4.674	5.822 ± 8.631	6.143 ± 4.427	29.425 ± 17.636	42.198 ± 24.055	13.130 ± 5.989		
δCe	0.999 ± 0.213	1.112 ± 0.150	1.091 ± 0.198	0.299 ± 0.082	0.930 ± 0.115	0.253 ± 0.038		
δEu	0.249 ± 0.150	0.472 ± 0.216	0.400 ± 0.294	0.763 ± 0.182	0.816 ± 0.769	0.589 ± 0.181		
LREE/HREE	1.088 ± 0.862	1.480 ± 0.908	1.523 ± 1.145	3.154 ± 0.978	5.562 ± 3.085	2.015 ± 1.229		
(La/Sm) _N	2.318 ± 1.962	1.738 ± 1.175	2.323 ± 1.844	4.746 ± 1.812	13.996 ± 3.674	3.037 ± 1.117		
(Gd/Lu) _N	1.855 ± 2.119	1.577 ± 1.393	3.088 ± 3.682	2.933 ± 1.219	1.227 ± 0.739	2.381 ± 1.315		

Note: Kruskal–Wallis Test, H value is Chi-square, p is progressive significance, significant level is 0.05, * means the difference was extremely significant. The details of cited data can be found in Table 1.

The following is an overview of the characteristics of the REEs in the present six nephrite origins.

The Xinjiang nephrite samples contain a very low abundance of REEs, ranging from 1.304 to 21.089 ppm (average ΣREE = 7.050 ppm). The chondrite-normalized REE patterns are characterized by obvious strong negative Eu anomalies ($\delta\text{Eu} = 0.027\sim 0.638$ (0.249)) and minor Ce anomalies ($\delta\text{Ce} = 0.566\sim 1.676$ (0.999)). Most samples show a horizontal seagull pattern with various degrees of fractionation between LREE and HREE, while fewer samples demonstrate a slightly right-leaning slope with a slight enrichment of LREE by $(\text{La}/\text{Sm})_N = 0.090\sim 9.001$ (2.318) and $(\text{Gd}/\text{Lu})_N = 0.133\sim 9.950$ (1.855).

The Qinghai nephrite samples have a lower total REE (ΣREE = 1.267~40.720 ppm, with an average of 5.822 ppm) and moderately Eu negative anomalies ($\delta\text{Eu} = 0.050\sim 0.874$ (0.472)). The chondrite-normalized REE patterns can reveal two different trends: partial samples are characterized by a flat pattern with no marked fractionation between LREE and HREE, while the other samples demonstrate a right-leaning slope with a light enrichment

of LREE relative to HREE by $LREE/HREE = 0.546\sim 3.667$ (1.480), $(La/Sm)_N = 0.308\sim 4.184$ (1.738), and $(Gd/Lu)_N = 0.176\sim 6.885$ (1.577).

The Russian nephrite samples have a lower abundance of REEs, ranging from 2.274 to 17.713 ppm (average $\Sigma REE = 6.143$ ppm). The chondrite-normalized REE patterns are characterized by various degrees of fractionation between LREE and HREE ($LREE/HREE = 0.115\sim 4.276$ (1.523)), slight enrichment of LREE, the overall decline of HREE ($(La/Sm)_N = 0.413\sim 6.225$ (2.323), $(Gd/Lu)_N = 0.068\sim 11.421$ (3.088)), and moderately Eu negative anomalies ($\delta Eu = 0.052\sim 1.103$ (0.400)).

The Luodian nephrite samples have a relatively higher abundance of REE ($\Sigma REE = 10.000\sim 95.910$ (29.425)). The chondrite-normalized REE patterns are uniform with an overall right slope with obvious enrichment of LREE ($LREE/HREE = 1.684\sim 5.896$ (3.154), $(La/Sm)_N = 2.648\sim 11.037$ (4.746), $(Gd/Lu)_N = 1.097\sim 6.056$ (2.933)), obviously negative Ce anomalies ($\delta Ce = 0.216\sim 0.644$ (0.299)), and relatively weak Eu negative anomalies ($\delta Eu = 0.474\sim 1.338$ (0.763)).

The Xiuyan nephrite samples have the highest abundance of REEs among the six origins ($\Sigma REE = 11.223\sim 98.469$ (42.198)). The chondrite-normalized REE patterns are characterized by obviously enriched LREE and flat HREE with a strong fraction between LREE and HREE ($LREE/HREE = 1.103\sim 11.732$ (5.556), $(La/Sm)_N = 6.161\sim 19.367$ (13.996), $(Gd/Lu)_N = 0.139\sim 3.039$ (1.227)). The patterns show overall moderately Eu negative anomalies ($\delta Eu = 0.209\sim 2.627$ (0.816)), but some samples reveal Eu positive anomalies.

The Dahua nephrite samples have an intermediate abundance of REEs among these six origins ($\Sigma REE = 3.870\sim 24.290$ (13.130)). The chondrite-normalized REE patterns are characterized by a relative enriched LREE and flat HREE ($LREE/HREE = 0.311\sim 3.828$ (2.015), $(La/Sm)_N = 1.167\sim 5.027$ (3.037), $(Gd/Lu)_N = 0.453\sim 4.614$ (2.381)), with strong Ce negative anomalies ($\delta Ce = 0.206\sim 0.325$ (0.253)), and moderately Eu negative anomalies ($\delta Eu = 0.291\sim 0.840$ (0.589)).

Nephrite chondrite-normalized REE patterns (Figure 2) show a tendency towards a certain regularity, although some variation occurs within some origins. According to the REE patterns, the six nephrite origins can be divided into three distinct groups: the Xinjiang–Qinghai–Russia group, the Luodian–Dahua group, and the Xiuyan group. Nephrite samples from Xiuyan are characterized by a high total amount of REE content and light rare earth enrichment, and some samples show positive Eu anomalies, distinguishing them from the other origins. The Luodian nephrite and the Dahua nephrite have a similar REE distribution pattern, with significant negative Ce anomalies and slight negative Eu anomalies, which can be used to distinguish them from the Xinjiang–Qinghai–Russia group, which has no significant Ce anomalies. Figure 3 exhibits the parameter scatter plots for REEs. As illustrated in Figure 3, the total abundance of REEs (ΣREE) and $(La/Sm)_N$ are significantly higher in Xiuyan nephrite than in those of the other origins; it is, therefore, possible to distinguish Xiuyan nephrite from the other nephrite sources with the help of binary diagrams (e.g., $(La/Sm)_N$ – ΣREE). In addition, the Luodian and Dahua origins have significant negative Ce anomalies, which can be clearly distinguished from the other origins using δCe – ΣREE binary diagrams. As expected, the REE parameter scatter matrix plot supports the natural grouping phenomenon demonstrated by the chondrite-normalized REE patterns. That is, these six origins can be divided into three different groups based on the chondrite-normalized REE patterns and the scatter matrix of the REE parameters.

3.2. Discriminant Analysis of Rare Earth Elements

3.2.1. Xinjiang–Qinghai–Russia Group

For the Xinjiang–Qinghai–Russia group, the origin discrimination model was developed using 14 REEs and linear discriminant analysis (LDA) to obtain the corresponding discriminant functions and group mass-center coordinates for the purpose of maximizing the separation of nephrite samples from three origins. The two functions explain 100% of the variance (Function 1 explains 69.3% of the total variance, and Function 2 explains 30.7%). Discriminant functions are shown as follows.

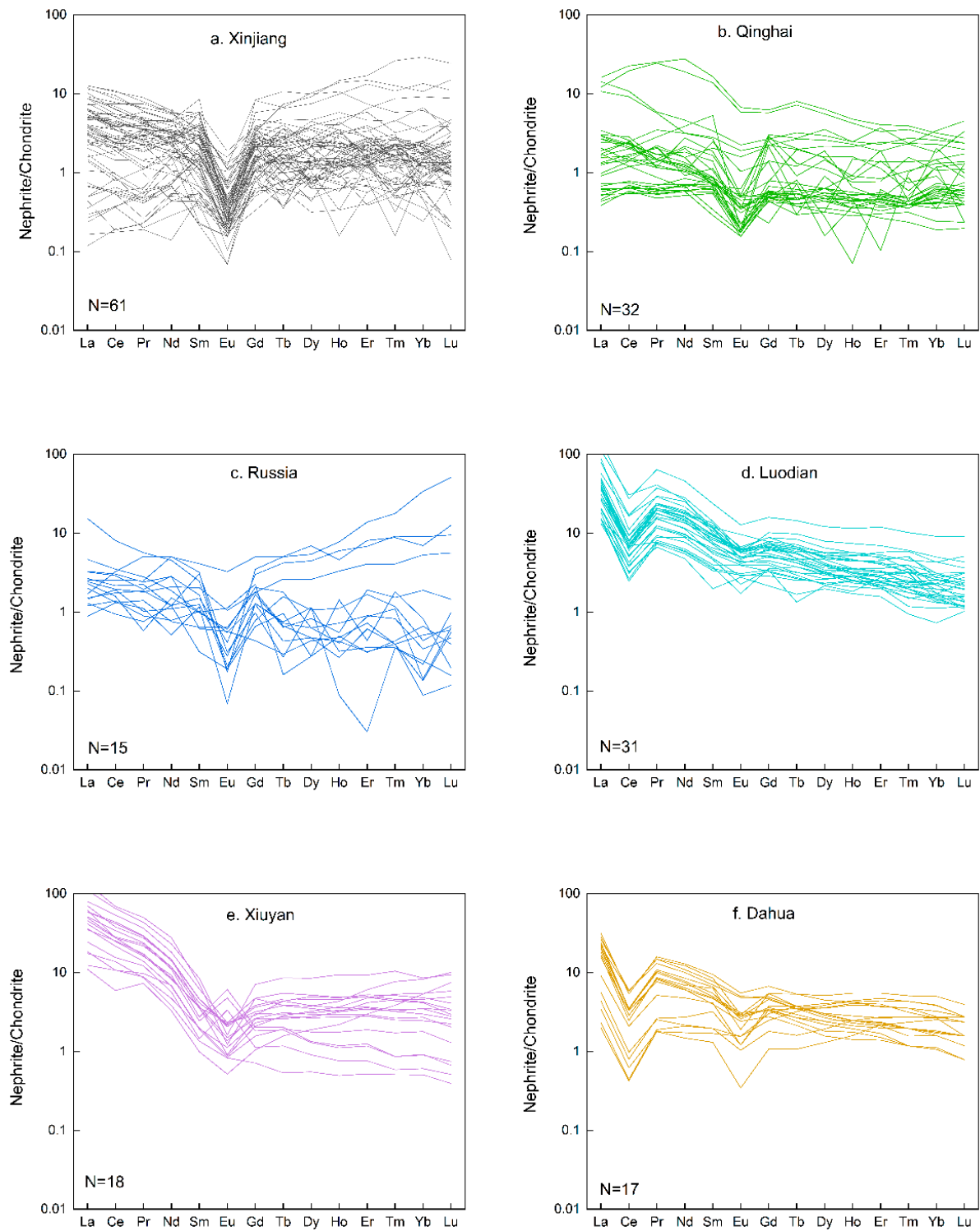


Figure 2. Chondrite-normalized REE patterns of nephrite from (a) Xinjiang, (b) Qinghai, (c) Russia, (d) Luodian, (e) Xiuyan, (f) Dahua. Normalizing values are from Sun and McDonough (1989) [51].

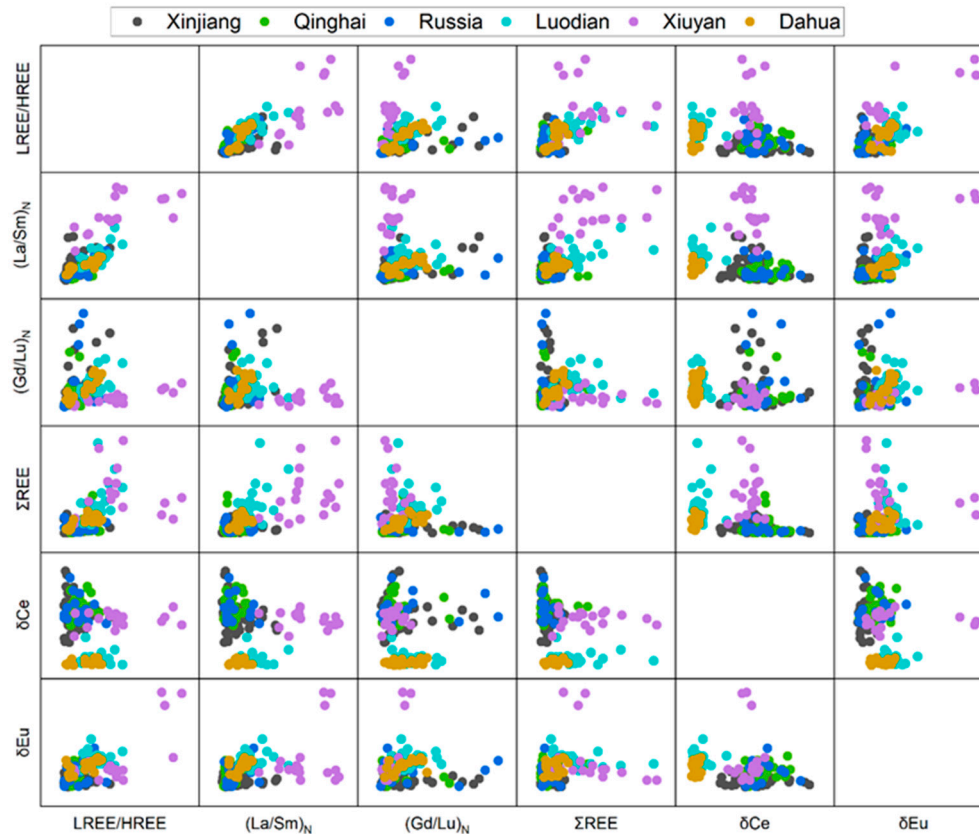


Figure 3. Scatter matrix of REE parameters of nephrite from different origins.

$$\begin{aligned} \text{DF1} = & 1.603\text{La} - 1.120\text{Ce} + 4.850\text{Pr} + 0.276\text{Nd} - 0.666\text{Sm} - 21.554\text{Eu} + \\ & 0.607\text{Gd} + 4.974\text{Tb} - 1.186\text{Dy} + 5.507\text{Ho} + 1.025\text{Er} + 3.054\text{Tm} - 0.845\text{Yb} - \\ & 2.063\text{Lu} - 0.598 \end{aligned} \quad (3)$$

$$\begin{aligned} \text{DF2} = & 1.551\text{La} - 0.827\text{Ce} + 0.299\text{Pr} + 0.052\text{Nd} - 0.856\text{Sm} + 10.261\text{Eu} + \\ & 1.913\text{Gd} + 1.495\text{Tb} - 1.005\text{Dy} - 7.179\text{Ho} + 0.508\text{Er} + 17.137\text{Tm} - 2.499\text{Yb} + \\ & 12.103\text{Lu} - 0.447 \end{aligned} \quad (4)$$

The data from the nephrite samples from Xinjiang, Qinghai, and Russia were visualized by plotting the two discriminant function scores (Figure 4). It is clear that the spatial separation of the nephrite samples from the three origins is close in proximity, and there is a wide range of overlapping data, which leads to difficulties in separating. To assess the reliability, the discriminant model was then validated by LOOCV. Because of severe data overlapping, the discriminant accuracy of some origins is poor. As shown in Table 3, the original accuracy of the discriminate model was 74.1%, and the cross-validation accuracy is 63.9%, indicating an unsatisfactory performance of this model for the classification of nephrite samples from these three origins. Specifically, Xinjiang nephrite can be distinguished from the other two origins with an accuracy of 96.7% in the original classification and 86.9% in cross-validation. Qinghai nephrite is distinguishable from Russian nephrite, but it is frequently misidentified as Xinjiang nephrite. Russian nephrite samples were easily misassigned to Xinjiang and Qinghai origins during classification, which heavily lowered the overall accuracy of the discrimination model. The poor performance of the LDA model indicates that the REEs composition alone is insufficient at differentiating the source of these origins. Other mutually complementary information (featured inclusions, spectral information, more chemical elements) may help to improve the discrimination accuracy.

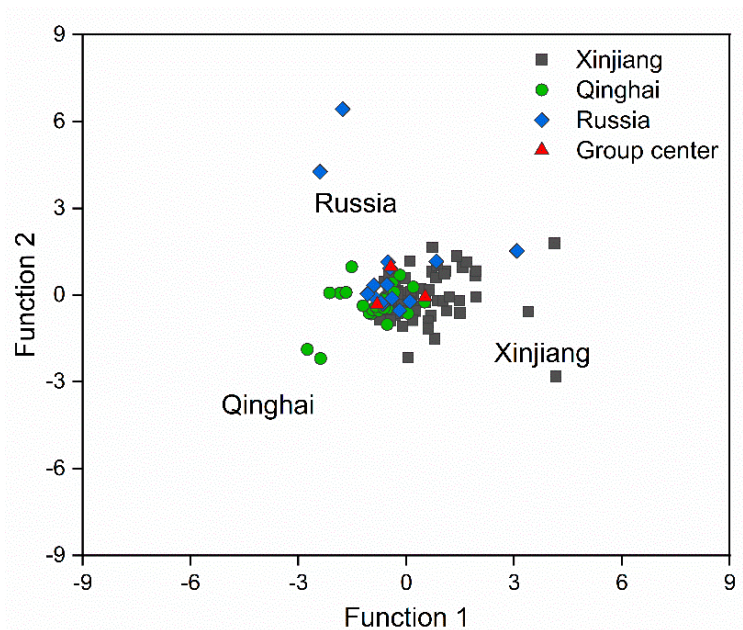


Figure 4. Scatter score plot of the LDA model of Xinjiang–Qinghai–Russia group in discriminating nephrite origin based on REEs.

Table 3. The predictive capacity of LDA model for Xinjiang–Qinghai–Russia group in discriminating geographical origins of nephrite samples based on REEs.

		Origins	Predicted Group Membership			Total Accuracy/%
			Xinjiang	Qinghai	Russia	
Original	Count	Xinjiang (n = 61)	59	2	0	74.1
		Qinghai (n = 32)	13	19	0	
		Russia (n = 15)	8	5	2	
	%	Discrimination accuracy/%	96.7	59.4	13.3	
Cross-validation	Count	Xinjiang (n = 61)	53	6	2	63.9
		Qinghai (n = 32)	16	15	1	
		Russia (n = 15)	8	6	1	
	%	Discrimination accuracy/%	86.9	46.9	6.7	

3.2.2. Luodian-Dahua Group

For the Luodian-Dahua group, linear discriminant analysis was also performed to establish a mathematical model for the classification of nephrite according to the origin based on REEs. Since two origins need to be distinguished, only one discriminant function was built. The discriminant function is shown as follows.

$$DF = -0.423La + 0.101Ce - 2.972Pr + 2.638Nd - 12.102Sm + 9.476Eu + 0.883Gd + 21.037Tb + 3.389Dy + 28.774Ho - 16.010Er - 10.745 - 9.340Yb + 95.271Lu - 1.661 \quad (5)$$

Figure 5 shows the relative frequency patterns of nephrite according to origin in a plot defined by the discriminant functions. The nephrite samples from Luodian and Dahua can be well separated in space, and the group mass centers were far away from each other, with only a small overlap. LOOCV was conducted to evaluate the predictive capacity of the discriminant model. The results of the validation are listed in Table 4; the original accuracy of the discriminate model was 97.9% and the cross-validation accuracy is 85.4%. These results indicate that the generated model can achieve good discrimination between the Luodian and Dahua origins.

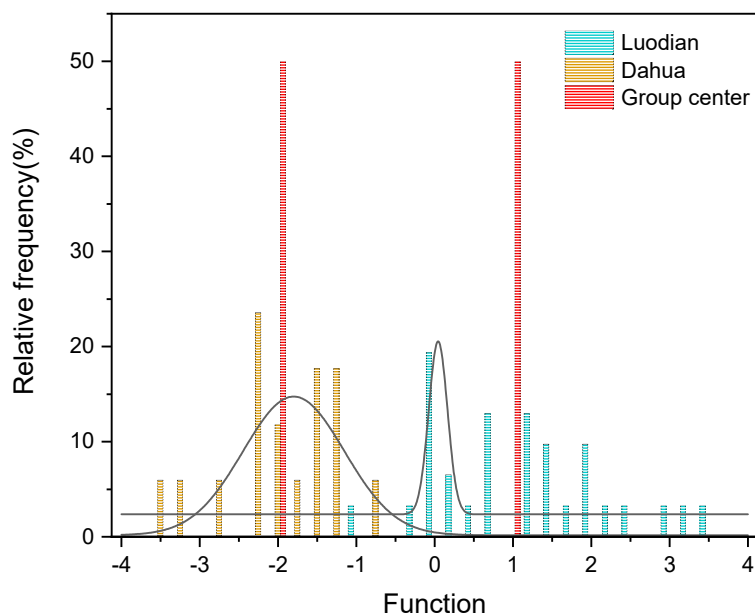


Figure 5. Relative frequency plot of the LDA model of Luodian–Dahua group in discriminating nephrite origin based on REEs.

Table 4. The predictive capacity of the LDA model for the Luodian-Dahua group in discriminating geographical origins of nephrite samples based on REEs.

		Origins	Predicted Group Membership		Total Accuracy/%
			Luodian	Dahua	
Original	Count	Luodian (n = 31)	30	1	97.9
	%	Dahua (n = 17)	0	17	
Cross-validation	Count	Discrimination accuracy / %	96.8	100	85.4
		Luodian (n = 31)	26	5	
	Dahua (n = 17)	2	15		
	%	Discrimination accuracy / %	83.9	88.2	

Note: 97.9% of the original grouped case was corrected and classified. 85.4% of the cross-validated grouped case was corrected and classified.

3.3. Geographic Origin Determination Scheme for Nephrite Based on REEs

A schematic of origin determination of nephrite is depicted in Figure 6. This approach can be briefly described as two steps. In the first step, by analyzing the 14 REE data sets, these nephrite origins were grouped broadly into three groups based on their chondrite-normalized REE patterns: the Xiuyan group, the Luodian-Dahua group, and the Xinjiang-Qinghai-Russia group. The samples from Xiuyan can be successfully identified in this step. In the second step, the LDA method is considered for further classification into their respective groups. For the Luodian-Dahua group, the LDA model performs well in separating, with an original classification accuracy of 97.9% and an 85.4% cross-validation accuracy, considering the closeness in ore genesis between the two origins. In contrast, for the Xinjiang–Qinghai–Russia group, the LDA model misclassifies due to heavily overlapping scatter scores.

Each sample goes through this procedure sequentially to determine its origin. Suppose a nephrite sample from Luodian is subjected to this schematic process, the first step by chondrite-normalized REE pattern categorizes it to Group 2. The sample continues to be discriminated by the LDA model in the second step and is then identified with an accuracy rate of 85.4%.

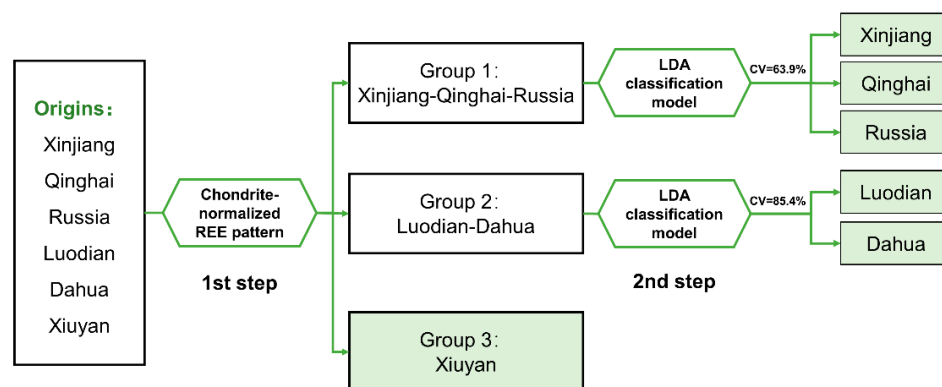


Figure 6. A schematic of origin determination of nephrite by REEs.

3.4. Interpreting the Performance of the Nephrite Origin Discriminant Model Based on REES from the Perspective of Metallogenic Genesis

The existence of differences in REE content between nephrites from different origins provides the basis for origin determination, enabling the further development of origin discrimination models. Previous studies indicated that the REE patterns of nephrite are primarily determined by the wall-rock composition, as well as hydrothermal fluids created by metallogenic processes [52]. In the present study, we attempt to discuss the petrogenesis of nephrite and derivation of nephrite-forming material in different origins, then explain the differences in REEs and verify the rationalization of the origin discrimination model.

Regarding the Xinjiang–Qinghai–Russia group, the nephrite deposits in Xinjiang are primarily distributed in the Kunlun Mountains along the southern end of the Tarim Basin and extend to the Altyn Tagh Mountain. Nephrite in this region was formed during the Hercynian orogeny period by metasomatism of Precambrian dolomitic marble with intrusive intermediate acid magmatic rocks (late Variscan, middle Variscan, and Caledonian granite) [2,37]. The Qinghai nephrite samples are also of dolomite-related metasomatism genesis. The wall rocks include dolomitic marble and banded siliceous dolomite from the Upper Proterozoic Wanbaogou Group, as well as dolomitic marble and gneiss from the Lower Proterozoic Jinshuikou Group. The intrusive rocks from the Early Triassic and the Permian contain intermediate-acid intrusive rocks, while those from the Late Carboniferous era contain intermediate-basic intrusive rocks [37]. Due to the characteristics of intrusive rocks, the REE patterns of Qinghai nephrite may exhibit some degree of variability. The dolomite-related nephrite deposits from Russia are located along the southern margin of the Siberian Craton, primarily in the Vitim region. The nephrite is a product of hydrothermal metasomatism between dolomitic marble and granitic melts, consisting of Qinghai and Xinjiang origins in ore genesis [6,7]. Geologically, Qinghai nephrite and Xinjiang nephrite have similar tectonic contexts, both being outcomes of metamorphism between magmatic rocks and carbonate rocks during the formation and evolution of the Kunlun orogenic belt [53], with the main differences being the lithology of the intrusive rocks and the ore-forming age. Although Russian nephrite is not in the same metallogenic belt as Xinjiang and Qinghai, a similar genesis of the deposits (both formed by contact metasomatism between dolomitic marble wall rocks and moderately acidic magmatic intrusive rocks) leads to an overall similar pattern of REEs in the three origins.

Regarding the Luodian–Dahua group, Luodian nephrite is considered as a long-term contact metasomatism genesis, and its wall rocks are diabase, silicalite, and dolomite limestone, while its intrusive rocks are diabase. It was also proven that the REEs of Luodian nephrite were not inherited from diabase, but were consistent with the stratigraphic silicalite, suggesting that diabase was not the main source of mineralization, only providing a thermodynamic condition [42,54]. The Dahua nephrite exists in the outer contact zone between diabase and carbonate rocks and its metallogenic genesis was identified as contact metasomatism [11]. The wall rocks are limestone, dolomitic limestone, and dolomite

intercalated with siliceous rock in Carboniferous Permian strata, and the intrusive rocks are gabbro or gabbro-diabase shallow basic intrusive rocks [11]. In terms of the source of minerogenic materials, the types of ore-forming parent rocks are consistent in their Luodian and Dahua origins. From the perspective of regional geology, considering that the geographical proximity of Dahua and Luodian origins are close and their metallogenic model is relatively consistent, it can be deduced that the two origins belong to another nephrite metallogenic belt in Southwest China.

Xiuyan nephrite mainly occurs in the contact zone of Proterozoic dolomite-marble in the Dashiqiao formation of the Liaohe Group, and its metallogenic genesis is regional metamorphism. Shallow marine facies dolomite was deposited in the Middle Early Proterozoic and later recrystallized to form the dolomitic marble in the late Early Proterozoic. At the end of the Early Proterozoic (about 1700 Ma), Si-rich hydrothermal water solution formed by regional metamorphism, and migmatization magma reacted with the surrounding rocks by hydrothermal metasomatism to form nephrite [10]. The unique distribution pattern of REEs in Xiuyan nephrite may be attributed to the old rock strata from the Early Proterozoic.

Overall, in light of the diversity of metallogenic genesis, REE contents and patterns differ across the various origins. Xinjiang–Qinghai–Russia group and Luodian–Dahua group are located in different tectonic plates and metallogenic belts. The differences in REE distribution patterns may be due to significant differences in metallogenic genesis. In terms of the performance of the models, the unsatisfactory prediction performance of the discriminant model of the Xinjiang–Qinghai–Russia group can be attributed to the geographical closeness and similarities in metallogenic parent rock, as well as metallogenic genesis.

4. Conclusions

This study proposes a novel approach to determine the origin of nephrite based on REEs measurements and the LDA method. REE contents and parameter ratios in nephrite are statistically different between the origins, with some geographical characteristics and origin identification. The six nephrite origins studied in this paper can be divided into three groups based on the chondrite-normalized REE patterns, namely the Xinjiang–Qinghai–Russia group, the Luodian–Dahua group, and the Xiuyan group, with significant differences between the groups, but not within the groups themselves. Xiuyan nephrite has its own unique chondrite-normalized REE pattern and can be well distinguished from other origins. The results of the LDA origin-determination model show the accuracy of the original classification and cross-validation for the Xinjiang–Qinghai–Russia group to be 74.1% and 63.9%, respectively, with strong overlap in discriminant score plots, causing difficulty in differentiation. This can be explained by geographical proximity and ore-forming genesis. The LDA origin-discrimination model for the Luodian–Dahua group has a 97.9% original classification accuracy and an 85.4% cross-validation accuracy, indicating a more accurate differentiation between the Luodian and Dahua origins.

At present, the databases for the origin determination of nephrite, both from our measurements and the literature collections, are currently insufficient. To develop an accurate origin determination model, the database needs to be expanded to eliminate errors caused by test methods and randomness in the testing process. From the performance of the LDA models, REEs as the only indicator for geographical origin determination is limited and other fingerprints must be added to further improve discrimination accuracy. Additionally, the lack of knowledge about the genesis of geological formations limits the theoretical progress of origin-determination methods, and a better understanding of the ore-forming genesis and geological context could better explain the differences between different nephrite origins.

Supplementary Materials: The following supporting information can be downloaded at: <https://www.mdpi.com/article/10.3390/min12111399/s1>, Table S1: Data results of rare earth element contents of nephrite samples from six origins.

Author Contributions: Conceptualization, Y.S.; methodology, Y.S.; software, Y.S.; writing—original draft preparation, Y.S.; writing—review and editing, M.Y.; supervision, M.Y. All authors have read and agreed to the published version of the manuscript.

Funding: This research was funded by the Center for Innovative Gem Testing Technology, China University of Geosciences, grant number CIGTXM-04-S202020. This research was supported by a grant from the Major Programs of the National Cultural Heritage Administration of China [The study of civilizational processes in the middle reaches of the Yangtze River (Xia, Shang and Zhou periods)], Heritage Protection Letter [2020] No. 444.

Data Availability Statement: Data is contained within the article or Supplementary Material.

Acknowledgments: This article cites test data from previously published papers. We would like to thank these contributors for their contributions.

Conflicts of Interest: The authors declare no conflict of interest.

References

1. Tang, Y.; Chen, B.; Jiang, R. *Chinese Hetian Nephrite, Xinjiang*; Xinjiang People's Publishing House: Xinjiang, China, 1994.
2. Liu, Y.; Deng, J.; Shi, G.; Yui, T.F.; Zhang, G.; Abuduwayiti, M.; Yang, L.; Sun, X. Geochemistry and petrology of nephrite from Alamas, Xinjiang, NW China. *J. Asian Earth Sci.* **2011**, *42*, 440–451. [[CrossRef](#)]
3. Gao, K.; Shi, G.; Wang, M.; Xie, G.; Wang, J.; Zhang, X.; Fang, T.; Lei, W.; Liu, Y. The Tashisayi nephrite deposit from South Altyn Tagh, Xinjiang, northwest China. *Geosci. Front.* **2019**, *10*, 1597–1612. [[CrossRef](#)]
4. Dong, B. Geological situation and characteristics of Qinghai nephrite from Golmud in Qinghai Province. *Geol. Build. Mater.* **1996**, *5*, 23–28.
5. Yu, H.; Wang, R.; Guo, J.; Li, J.; Yang, X. Study of the minerogenetic mechanism and origin of Qinghai nephrite from Golmud, Qinghai, Northwest China. *Sci. China Earth Sci.* **2016**, *59*, 1597–1609. [[CrossRef](#)]
6. Burtseva, M.V.; Ripp, G.S.; Posokhov, V.F.; Zyablitshev, A.Y.; Murzintseva, A.E. The sources of fluids for the formation of nephritic rocks of the southern folded belt of the Siberian Craton. *Dokl. Earth Sci.* **2015**, *460*, 82–86. [[CrossRef](#)]
7. Burtseva, M.V.; Ripp, G.S.; Posokhov, V.F.; Murzintseva, A.E. Nephrites of East Siberia: Geochemical features and problems of genesis. *Russ. Geol. Geophys.* **2015**, *56*, 402–410. [[CrossRef](#)]
8. Yui, T.F.; Kwon, S.T. Origin of a dolomite-related jade deposit at Chuncheon, Korea. *Econ. Geol.* **2002**, *97*, 593–601. [[CrossRef](#)]
9. Wang, S.; Duan, T.; Zheng, Z. Mineralogical and petrological characteristics of Xiuyan nephrite and its minerogenetic model. *Acta Petrol. Mineral.* **2002**, *21*, 79–90.
10. Wang, S.; Zhao, C.; Yu, G.; Yun, X.; Duan, T. *Xiuyan Jades in China*; Science Press: Beijing, China, 2007.
11. Wang, S.; Yu, G.; Wang, C.; Fan, G.; Mo, Y.; Yu, X.; Li, X.; Xu, L.; Li, X. *Dahua Jades in China*; Science Press: Beijing, China, 2016.
12. Yin, Z.; Jiang, C.; Santosh, M.; Chen, Y.; Bao, Y.; Chen, Q. Nephrite jade from Guangxi Province, China. *Gems Gemol.* **2014**, *50*, 228–235. [[CrossRef](#)]
13. Yang, L.; Lin, J.; Wang, L.; Tan, J.; Wang, B. Petrochemical Characteristics and Genesis Significance of Luodian Jade from Guizhou. *J. Mineral. Petrol.* **2012**, *32*, 12–19. [[CrossRef](#)]
14. Ling, X.; Schmädicke, E.; Wu, R.; Wang, S.; Gose, J. Composition and distinction of white nephrite from Asian deposits. *Neues Jahrb. Mineral. Abh.* **2013**, *190*, 49–65. [[CrossRef](#)]
15. Luo, Z.; Yang, M.; Shen, A.H. Origin Determination of Dolomite-Related White Nephrite through Iterative-Binary Linear Discriminant Analysis. *Gems Gemol.* **2015**, *51*, 300–311. [[CrossRef](#)]
16. Wang, Y.; Yuan, X.; Shi, B.; Zhang, Q.; Chen, T. Origins of nephrite by laser-induced breakdown spectroscopy using partial least squares discriminant analysis. *Chin. J. Lasers* **2016**, *43*, 1211001. [[CrossRef](#)]
17. Yu, J.; Hou, Z.; Sheta, S.; Dong, J.; Han, W.; Lu, T.; Wang, Z. Provenance classification of nephrite jades using multivariate LIBS: A comparative study. *Anal. Methods* **2018**, *10*, 281–289. [[CrossRef](#)]
18. Chen, D.; Pan, M.; Huang, W.; Luo, W.; Wang, C. The provenance of nephrite in China based on multi-spectral imaging technology and gray-level co-occurrence matrix. *Anal. Methods* **2018**, *10*, 4053–4062. [[CrossRef](#)]
19. Xu, H.; Lin, L.; Li, Z.; Huang, M.; Zhou, Z. Nephrite Origin Identification Based on Raman Spectroscopy and Pattern Recognition Algorithms. *Acta Opt. Sin.* **2019**, *39*, 0330001. [[CrossRef](#)]
20. Gu, A.; Luo, H.; Yang, X. Feasibility study on nondestructive methods for identification of the origin of nephrite based on near-infrared spectroscopy and chemometrics. *Sci. Conserv. Archaeol.* **2015**, *27*, 78–83. [[CrossRef](#)]
21. Yang, T.; Wang, X.; Huang, B.; Zang, Z.; Wang, J.; Yan, S. Origin identification of white nephrite based on terahertz time-domain spectroscopy. *Acta Petrol. Mineral.* **2020**, *39*, 314–322.
22. Gao, K.; Fang, T.; Lu, T.; Lan, Y.; Zhang, Y.; Wang, Y.; Chang, Y. Hydrogen and Oxygen Stable Isotope Ratios of Dolomite-Related Nephrite: Relevance for its Geographic Origin and Geological Significance. *Gems Gemol.* **2020**, *56*, 266–280. [[CrossRef](#)]
23. Zhang, H.; Gao, S. *Geochemistry*; Geological Publishing House: Beijing, China, 2012.
24. Luo, Y.; Liu, Y.; Hu, S.; Gao, S. Rare earth elements analysis of geological samples by LA-ICP-MS. *Earth Sci. J. China Univ. Geosci.* **2001**, *26*, 508–512.

25. Abduriyim, A.; Kitawaki, H. Applications of laser ablation-inductively coupled plasma-mass spectrometry (LA-ICP-MS) to gemology. *Gems Gemol.* **2006**, *42*, 98–118. [[CrossRef](#)]
26. Ma, G.; Zhang, Y.; Zhang, J.; Wang, G.; Chen, L.; Zhang, M.; Liu, T.; Liu, X.; Lu, C. Determining the geographical origin of Chinese green tea by linear discriminant analysis of trace metals and rare earth elements: Taking Dongting Biluochun as an example. *Food Control* **2016**, *59*, 714–720. [[CrossRef](#)]
27. Cerutti, C.; Sánchez, R.; Sánchez, C.; Ardini, F.; Grotti, M.; Todolí, J.L. Prospect on rare earth elements and metals fingerprint for the geographical discrimination of commercial Spanish wines. *Molecules* **2020**, *25*, 5602. [[CrossRef](#)]
28. Farmaki, E.G.; Thomaidis, N.S.; Minioti, K.S.; Ioannou, E.; Georgiou, C.A.; Efstathiou, C.E. Geographical Characterization of Greek Olive Oils Using Rare Earth Elements Content and Supervised Chemometric Techniques. *Anal. Lett.* **2012**, *45*, 920–932. [[CrossRef](#)]
29. Joebstl, D.; Bandoniene, D.; Meisel, T.; Chatzistathis, S. Identification of the geographical origin of pumpkin seed oil by the use of rare earth elements and discriminant analysis. *Food Chem.* **2010**, *123*, 1303–1309. [[CrossRef](#)]
30. Aceto, M.; Musso, D.; Calà, E.; Arièri, F.; Oddone, M. Role of Lanthanides in the Traceability of the Milk Production Chain. *J. Agric. Food Chem.* **2017**, *65*, 4200–4208. [[CrossRef](#)]
31. Drivelos, S.A.; Danezis, G.P.; Halagarda, M.; Popek, S.; Georgiou, C.A. Geographical origin and botanical type honey authentication through elemental metabolomics via chemometrics. *Food Chem.* **2021**, *338*, 127936. [[CrossRef](#)]
32. Xiang, F.; Cheng, W.; Zhen, J.G.; Zhang, Q.; Li, K.; Liu, J. Rare-Earth Element Characters of Jewels of Jinsha Site in Chengdu and Its Significance for Indicating Material Source. *J. Earth Sci. Environ.* **2008**, *30*, 54–56. [[CrossRef](#)]
33. Ye, S.; Li, L.; Wang, J.; Li, R.; Cheng, L.; Lu, S. Rare earth concentration and provenance of ancient porcelain fired in Hutian Kiln, Jiangxi Province. *J. Chin. Rare Earth Soc.* **2014**, *32*, 507–512. [[CrossRef](#)]
34. She, L.; Qin, Y.; Luo, W.; Huang, F.; Li, T. Provenance tracing of Turquoise in Northwest Hubei Using Rare Earth Elements. *Chin. Rare Earths* **2009**, *30*, 59–62.
35. Zhong, Y.; Qiu, Z.; Li, L.; Gu, X.; Luo, H.; Chen, Y.; Jiang, Q. REE composition of nephrite jades from major mines in China and their significance for indicating origin. *J. Chin. Soc. Rare Earth* **2013**, *31*, 738–748.
36. Siqin, B.; Qian, R.; Zhuo, S.; Gao, J.; Jin, J.; Wen, Z. Studies of rare earth elements to distinguish nephrite samples from different deposits using direct current glow discharge mass spectrometry. *J. Anal. At. Spectrom.* **2014**, *29*, 2064–2071. [[CrossRef](#)]
37. Yu, H. Coloring and Metallogenic Mechanisms of Different Colors in Qinghai Nephrite. Ph.D. Thesis, Nanjing University, Nanjing, China, 2016.
38. Ling, X.; Wu, R.; Wang, S.; Ding, Z.; Shi, W. A Study on Coloration Mechanism of Qinghai Green Nephrite by LA-ICP-MS. In Proceedings of the 2009 China Gems & Jewelry Academic Conference, Beijing, China, 3 November 2009; pp. 186–190.
39. Ling, X.; Wu, R.; Schmadicke, E.; Gose, J.; Wang, S. Chemical composition and color of lilac gray tremolite jade from Qinghai Province. In Proceedings of the International Symposium on Jade, Beijing, China, 1–2 September 2011; pp. 105–114.
40. Liao, Z.; Zhi, Y. *Study on Nephrite from Luodian, Guizhou Province*; China University of Geosciences Press: Wuhan, China, 2017.
41. Zhang, Y.; Yang, R.; Gao, J.; Chen, J.; Liu, Y.; Zhou, Z. Geochemical characteristics of nephrite from Luodian County, Guizhou Province, China. *Acta Mineral. Sin.* **2015**, *35*, 56–64.
42. Li, K.; Jiang, T.; Xing, L.; Zhou, M.; Luo, T. A Preliminary Study on Mineralogy and Ore Deposits Genetical Model of Luodian Nephrite Jade, Luodian, Guizhou Province, China. *Acta Mineral. Sin.* **2014**, *34*, 223–233.
43. Che, Y. Gemology and Mineralogy Study on Luodian Nephrite. Master's Thesis, China University of Geosciences, Beijing, China, 2013.
44. Liu, Y.; Hu, Z.; Gao, S.; Günther, D.; Xu, J.; Gao, C.; Chen, H. In situ analysis of major and trace elements of anhydrous minerals by LA-ICP-MS without applying an internal standard. *Chem. Geol.* **2008**, *257*, 34–43. [[CrossRef](#)]
45. Fisher, R.A. the Use of Multiple Measurements in Taxonomic Problems. *Ann. Eugen.* **1936**, *7*, 179–188. [[CrossRef](#)]
46. Masuda, A.; Nakamura, N.; Tanaka, T. Fine structures of mutually normalized rare-earth patterns of chondrites. *Geochim. Cosmochim. Acta* **1973**, *37*, 239–248. [[CrossRef](#)]
47. Dołęgowska, S.; Migaszewski, Z.M. Anomalous concentrations of rare earth elements in the moss-soil system from south-central Poland. *Environ. Pollut.* **2013**, *178*, 33–40. [[CrossRef](#)]
48. Evensen, N.M.; Hamilton, P.J.; O'Nions, R.K. Rare-earth abundances in chondritic meteorites. *Geochim. Cosmochim. Acta* **1978**, *42*, 1199–1212. [[CrossRef](#)]
49. Boynton, W.V. Cosmochemistry of the rare earth elements: Meteorite studies. *Dev. Geochem.* **1984**, *2*, 63–114. [[CrossRef](#)]
50. Taylor, S.R.; McLennan, S.M. *The Continental Crust: Its Composition and Evolution. An Examination of the Geochemical Record Preserved in Sedimentary Rocks*; Blackwell Science: Oxford, UK, 1985.
51. Sun, S.S.; McDonough, W.F. Chemical and isotopic systematics of oceanic basalts: Implications for mantle composition and processes. *Geol. Soc. Spec. Publ.* **1989**, *42*, 313–345. [[CrossRef](#)]
52. Yu, H.; Jia, Z.; Lei, W. Study on Geochemical Characteristics and Influencing Factors of Rare Earth Elements in Chinese Nephrite. *Mod. Min.* **2019**, *3*, 13–17.
53. Li, Y.; Liao, Z.; Shi, X. The Comparison Study between Qinghai Nephrite and Xinjiang Nephrite. *Shanghai Geol.* **2002**, *8*, 58–61.
54. Fan, E.; Lan, Y.; Dai, Z.; Wang, H.; Li, L. Geological Features of Luodian Tremolite Deposit, Guizhou Province, China and Its Prospecting Prediction. *Acta Mineral. Sin.* **2012**, *32*, 304–309. [[CrossRef](#)]